


Article

Decomposition Characteristics of SF₆ under Flashover Discharge on the Epoxy Resin Surface

Hao Wen ^{1,2}, Xiaoxing Zhang ^{1,*} , Rong Xia ³, Guoxiong Hu ¹ and Yunjian Wu ¹

¹ School of Electrical Engineering, Wuhan University, Wuhan 430072, China; wenhao198711@163.com (H.W.); 15733221344@163.com (G.H.); wuyunjian@whu.edu.cn (Y.W.)

² State Grid Electric Power Research Institute, Wuhan Nari Co Ltd, Wuhan 430074, China

³ Wuhan Branch, China Electric Power Research Institute Co., Ltd., Wuhan 430074, China; xiarong@epri.sgcc.com.cn

* Correspondence: xiaoxing.zhang@outlook.com; Tel.: +86-136-2727-5072

Received: 6 March 2019; Accepted: 25 April 2019; Published: 30 April 2019



Abstract: In this paper, the flashover discharging experiment was carried out on epoxy resin surface in an SF₆ atmosphere under pin-plate electrodes, with the electrodes distance from 5 mm to 9 mm. The concentration of seven characteristic gases was detected, indicating that the concentration of SOF₂ and CF₄ was the two highest, followed by SO₂, CO₂, SO₂F₂, CS₂, and H₂S. Based on the changes in the concentration of the characteristic gases, a preliminary rule was proposed to predict the occurrence of flashover discharge on epoxy resin: When the concentration of SOF₂ reaches twice of CF₄ concentration, and the total concentration of both SOF₂ and CF₄ is much higher than that of H₂S, a possible flashover discharge on the epoxy resin surface in SF₆-infused electrical equipment occurs. Through the simulation of decomposition of epoxy resin, it has been revealed that H₂O has different generation paths that can facilitate the formation of SOF₂, finally influencing the concentration variation of the seven characteristic gases.

Keywords: flashover discharge; SF₆ decomposition; epoxy resin; characteristic gases

1. Introduction

Gas-insulated electrical equipment has been widely used in power system because of their advantages such as compact size, high reliability, and a long maintenance period [1,2]. It was found that a considerable proportion of the internal faults of GIS (gas insulated switchgear) are closely related to the insulating spacer used to support the copper conductor, among which the surface discharge of insulating spacer is hard to be detected due to its randomness and instantaneity [3,4]. So far, attention has been paid to the fault detection technology for insulating spacer. The monitoring system on the decomposed gases of SF₆ develops rapidly, which provides an effective way to judge the operation situation of SF₆-infused electrical equipment.

SF₆ can decompose into a series of subfluorides and sulfides when high energy imposes on SF₆ molecules on the condition of partial discharge, overheating, corona, electrical breakdown, or even ultraviolet radiation [5–7]. Conventionally, subfluorides can recombine with fluorine to form SF₆ molecules again, owing to the intrinsic electronegativity property of SF₆. However, in most cases, air and water vapor mixed with SF₆ exists. These impurities react with subfluorides and produce various gases like SOF₄, SOF₂, SO₂F₂, SF₄, SO₂, CF₄, CO₂, H₂S, and so on [8–10], which prevent the recombination of SF₆ and subsequently reduce its insulation strength. Based on the concentration variation, a preliminary fault diagnosis method was provided to judge running situation of electrical equipment [8–10]. However, given the complicated internal situation of electrical equipment, there are many influential factors that tend to make concentration of decomposition components from SF₆

fluctuate drastically, such as temperature, humidity, and running voltage. Flashover discharge on the surface of epoxy resin gives rise to partial decomposition of epoxy resin, leading to potential chemical reaction between epoxy resin and SF₆ decomposition byproducts. However, this critical influential factor on SF₆ byproduct concentration attracts less attention today.

The decomposition of SF₆ has been extensively studied. Sausers et al. [11] conducted experiments on the effect of oxygen on SF₆ decomposition byproducts and found that oxygen can promote the production of SO₂F₂ and SOF₄, which has little effect on the generation rate of SOF₂. Derdouri et al. [12] designed a study on the SF₆ decomposition products when water vapor exists and found that SOF₂ and SO₂F₂ generate stably in existence of water vapor. Later, it was found that SF₆ decomposition byproducts, including SOF₄, SOF₂, SO₂F₂, SO₂, HF, would appear as long as water vapor and oxygen existed [13]. Additionally, a study reported that several SF₆ decomposition byproducts under four different kinds of partial discharge models, showing that CF₄, CO₂, SO₂F₂, SOF₄, SOF₂, SO₂, and H₂S were main decomposition products of SF₆, among which the content of SOF₂ and SO₂F₂ were the highest [14]. Furthermore, Belmadani et al. [15] explored the characteristics of SF₆ decomposition products under AC arc and pointed out that the total content of SOF₂ and SO₂ would increase with current intensity. It has been generally accepted that all SF₆ decomposition products concentration would increase with discharge energy, regardless of the kind of discharge [16–18]. The influences of solid insulation material on the decomposition of SF₆ were also studied. For example, it was reported that CF₄ would appear [12], since organic materials contain abundant C-H bonds that can easily react with fluorine under high-energy arc discharge. Afterward, a small amount of CS₂ was detected when flashover discharges happened on epoxy resin surface in 110 kV GIS, thus making it a characteristic gas in a fault detection system [19]. There is no dispute that SOF₂, SO₂F₂, and SO₂ will occur easily in partial discharge situation, and that H₂S would be generated when discharge energy is high enough. Moreover, CF₄, CO₂, and CS₂ would be generated when organic solid insulation materials decomposed partially under high voltage [12,15].

So far, no report has focused on how epoxy resin affects the decomposition of SF₆ under flashover discharge yet. Additionally, it is too complicated to elaborate the chemical mechanism behind it. Although thermal and mechanical of epoxy resin can be enhanced through incorporating some filler into the polymer matrix, it still can decompose under arc discharge [20–22]. In the current study, pin-plate electrodes on the epoxy resin insulation spacer surface were designed; flashover discharge at different distances of pin-plate electrodes was carried out; and the concentration of decomposition byproducts of SF₆, including SOF₂, SO₂F₂, SO₂, H₂S, CF₄, CO₂, and CS₂, was examined in order to find the relationship between decomposition of SF₆ under flashover discharge on the epoxy resin surface. Besides, by simulating decomposition process of epoxy resin, the generation path of each gas was revealed.

2. Materials and Methods

2.1. Materials

In the present study, the bisphenol-A epoxy resin E51 (DGEBA) was purchased from Wuxi Lan-Star Petrochemical Co., Ltd. (Wuxi, China). Epoxy resin was cured by an amine curing agent consisting of an adduct of diethylenetriamine and butyl glycidyl ether, known as 593 curing agent, supplied by Wuhan Shen Chemical Reagents and Equipments Co., Ltd. (Wuhan, China). High-precision SF₆ gas with grade of purity of 99.999% was supplied by Wuhan Newradar Gas Co., Ltd. (Wuhan, China). Therefore, the original percentage content of O₂ and H₂O in the gas was low enough to be omitted.

2.2. Experiment Platform

Among a multitude of documented electrical faults, flashover in the electrical equipment happens frequently. Today flashover fault can be detected easily, but it is still hard to explain the complicated mechanism behind it [5–7]. Flashover discharge emphasizes on electrical breakdown of gap happening

on solid material surface, such as flashover discharge on basin spacer surface in gas-insulated electrical equipment, where flashover voltage or flashover current was studied. Therefore, in our experiment, pin-plate electrodes on the epoxy resin surface was devised to investigate influence of surface breakdown of epoxy resin on SF₆ decomposition byproducts category and their concentration.

To create a severely uneven electrical field, pin-plate electrodes were used in this study, as shown in Figure 1. Given that the conducting rod in high-voltage cable is made of copper with better electric conductivity, the positive electrode in our study was a long-customized needle made of copper, the curvature radius of the needle electrode is 0.5 mm and beveled at 30° on the sample surface. The plate electrode is a semicircle copper sheet with a diameter of 10 mm and is stuck to the surface of epoxy resin with a small amount of conductive silver paste to ensure that the electrical arc was close enough to the surface when the gap breaks down. The epoxy spacer sample is a square piece with a size of 50 mm × 50 mm × 2 mm. The pin-plate electrodes are positioned in a sealed cylinder made of polymethyl methacrylate (PMMA) as shown in Figure 2. The AC high voltage power can provide a maximum value of 50 kV. Concentration of decomposed components of SF₆ was measured on the gas chromatograph-mass spectrometer (GC-MS) and the type of GC-MS is Shimadzu QP-2010Ultra (Shimadzu Co., LTD, Kyoto, Japan).

To protect the voltage divider, the value of R2 in Figure 2 was usually below 200 Ω, and the value of R1 was usually above 3000 Ω to protect the transformer when voltage divider was totally destroyed. Because epoxy resin has a high electrical resistivity with an order of magnitude above 10¹³ Ω cm, it is fully accepted that the break-down voltage on the sample surface equals to the highest shown value on the operating board when the gap was not broken down.

Because roughness of sample surface has a significant influence on flashover discharge property of epoxy resin, roughness of the samples was assessed on the Surface Profilometer 2300 supplied by Wale Electromechanical Technology Co., Ltd. (Xi'an, China). Roughness of all the epoxy resin samples had an average value of 0.35 μm in the range from 0.27 μm to 0.48 μm. Conventionally, roughness of solid material surface should be kept below 1 μm in order to ensure the AC (Alternating Current) arc creeping closely on the sample surface.

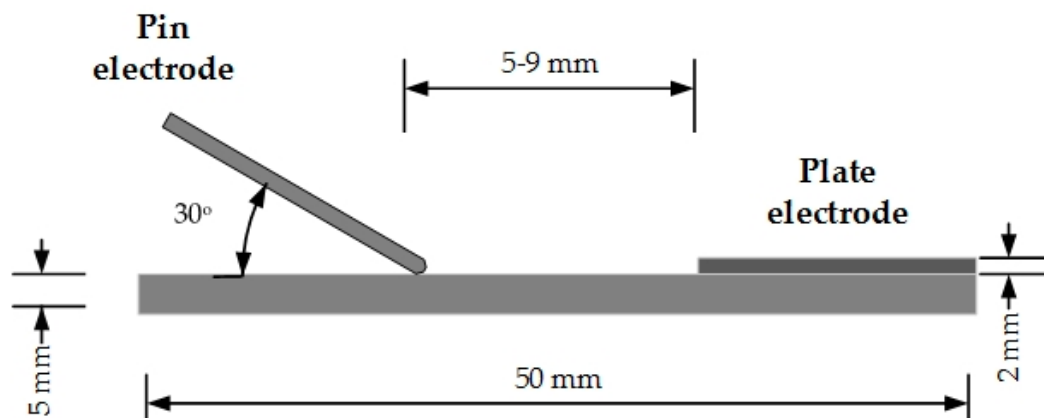


Figure 1. Pin-plate electrodes on epoxy resin.

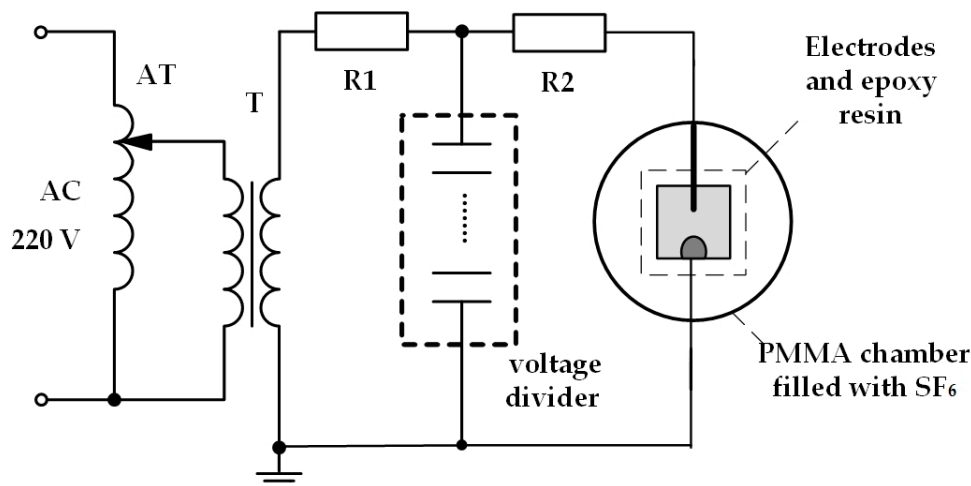


Figure 2. AC experimental equipment.

2.3. Experiment Procedures

The specific experimental procedures are listed as follows:

First, all experiment materials were cleaned with anhydrous ethanol to get rid of dust and other impurities that may adhere to the experiment materials. After being volatilized with anhydrous ethanol, the epoxy spacer and electrodes were placed in the fixed position in the container. The distance between the pin-plate electrodes was set at 5, 6, 7, 8 and 9 mm, respectively. Then, the container was sealed.

Second, the chamber was evacuated to 0.01 MPa and filled with fresh SF₆ until the pressure reached 0.2 MPa. It needed to take three times to remove most of water vapor and air. Subsequently, 100 mL of gas was extracted as the initial reference.

Finally, voltage was imposed slowly at the rate of 2 kV/30 s until the gap between the electrodes broke down, then the discharge voltage was recorded. After the decomposed gases diffused for 3 min in the chamber, 100 mL of gas was extracted from the chamber and then injected into the GC-MS. Twenty-one flashover discharge times were conducted for each gap distance in order to find the basic growth law of SF₆ decomposition byproducts. As we all know, the surface flashover does significant harm to the dielectric property of epoxy resin. As the discharge number increased, the flashover voltage decreased slowly. The small decomposition, or the carbonization of the epoxy resin surface can cause obvious characteristic gases concentration change [23]. Therefore, 21 times of flashover discharges are enough to make significant harm to dielectric properties of epoxy resin and create more precise concentration variation.

3. Results and Discussion

3.1. Discharge Voltages Comparison

Figure 3 shows initial flashover discharge voltages vs. discharge times at different pin-plate electrodes distances. It is apparent that discharge voltage decreased rapidly in the first three times flashover discharges. Then, discharge voltage fluctuated slowly in a downward trend on the whole. After the breakdown of the gap between the electrodes, roughness of the epoxy resin sample surface increased with an obvious carbonization trace, which would greatly reduce flashover discharge voltage under the uneven electrical field. At the same time, water vapor generating during the decomposition of epoxy resin could also enhance the conductivity of carbonized trace on the surface [24]. As a result, the flashover discharge voltage decreased in the first three times. However, the roughness of the sample surface did not markedly change after being discharged four to six times, and water vapor maintained at a relatively stable level because it was exhausted quickly after it was generated. Hence, the flashover discharge voltage fluctuated in a downward trend.

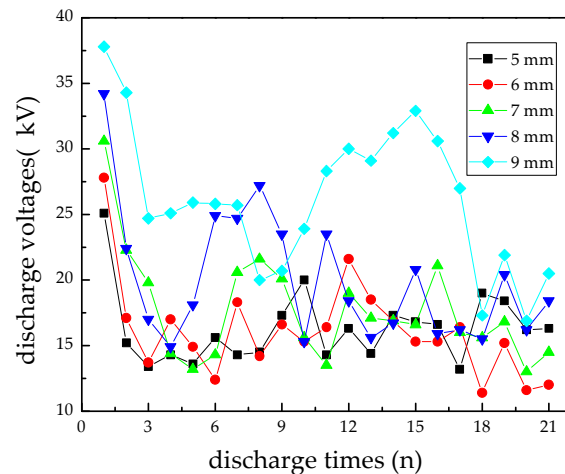


Figure 3. Initial flashover discharge voltages vs. discharge times at different pin-plate electrodes distances.

A longer distance between the electrodes could cause a higher discharge voltage in the first three times, but longer distances cannot guarantee a higher discharge voltage as the discharge continued. In Figure 3, by keeping the distance of pin-plate electrodes at 9 mm, the flashover voltage increased slowly from 10 to 15 times flashover discharges, which can be attributed to the randomness of flashover discharge and surface structure change. A longer gap distance led to greater dispersion of discharge voltage, creating more arc discharge channels among which the actual surface creepage distance was longer than 9 mm (Figure 4). In Figure 4a, the flashover distance was obviously larger than 9 mm, while the creepage distances in Figure 4b,c were a little shorter. Mostly, the creepage distances were all above 9 mm in which the surface structure played an important role in the development direction of electrical tree. Compared with discharging at shorter gap distances, the electrical tree may develop in more directions at the gap distance of 9 mm, leading to more fluctuating flashover discharge voltages.

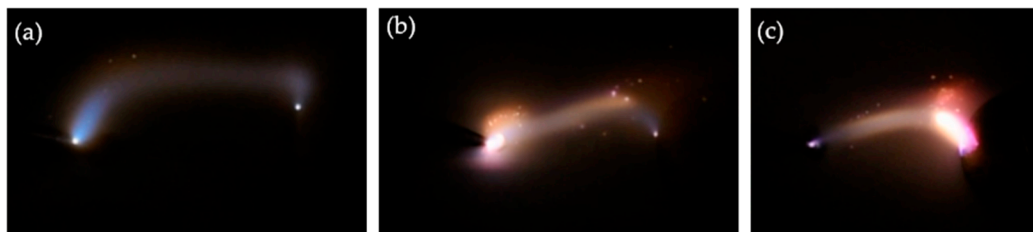


Figure 4. Digital images showing randomness of creepage distance at the gap distance of 9 mm.

The surface roughness of the epoxy resin samples before flashover discharge had an average value of 0.35 μm . After 21 times discharges, there generated several visible carbonized traces, so the roughness around the traces on the samples were measured to assess the decomposition extent of epoxy resin at different gap distances. The average roughness of the epoxy resin samples after 21 times discharges was shown in Table 1.

Table 1. Average roughness of the epoxy resin samples after 21 times flashover discharges at different pin-plate electrodes distances.

Gap Distances (mm)	5	6	7	8	9
Roughness/ (μm)	0.7	0.761	0.859	0.807	0.887

It was reported that with the accumulation of aging energy on the material surface, the particles formed on the material surface were increased both in number and size, leading to the growth of surface roughness; and, the break of the molecular chains of epoxy resin on the surface resulted in oxidation

and carbonization [25]. Increased roughness can also result in larger fluctuation of break-down voltages. Taken together, average roughness should be kept in a reasonable range for ensuring the arc creeping to be closely enough to the surface.

3.2. Concentration Variation of Seven Characteristic Gases

Figure 5 shows the concentration of the seven characteristic gases (CF_4 , CO_2 , SO_2F_2 , SOF_2 , H_2S , SO_2 , and CS_2) vs. discharge times at different pin-plate electrodes distances. The results showed a tendency that all gases concentration increased steadily with the increase of flashover discharge times. It is obvious that the concentration of SOF_2 and CF_4 was the highest while the concentration of other gases was relatively lower, especially SO_2F_2 , CS_2 , and H_2S . Taken together, the concentration of the seven characteristic gases follows the following order: $\text{SOF}_2 > \text{CF}_4 > \text{SO}_2 > \text{CO}_2 > \text{SO}_2\text{F}_2 > \text{CS}_2 > \text{H}_2\text{S}$.

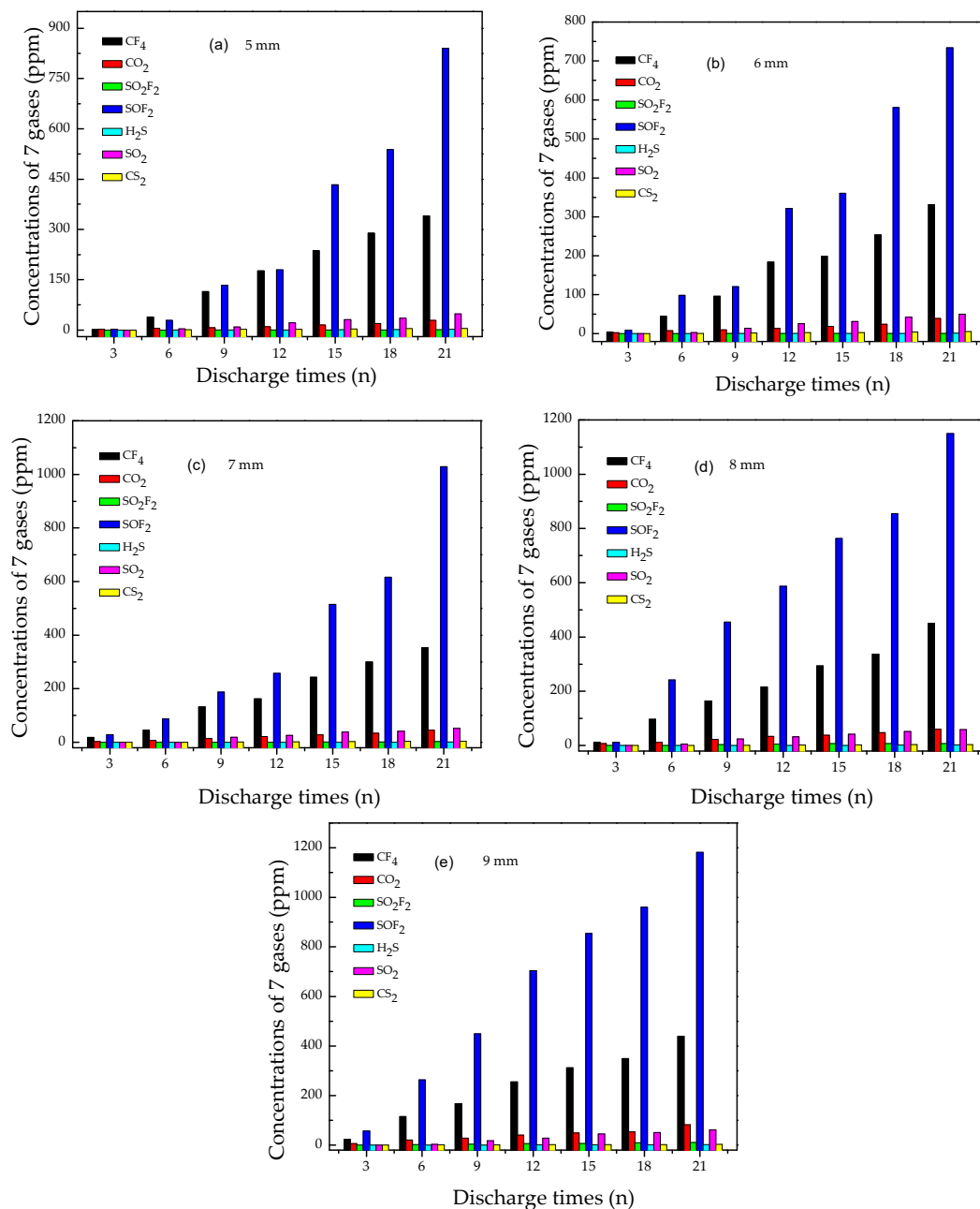


Figure 5. Concentration of seven gases vs. discharge times at different pin-plate electrodes distances. (a) 5 mm, (b) 6 mm, (c) 7 mm, (d) 8 mm, and (e) 9 mm.

At the pin-plate electrodes distance of 5 mm, after flashover discharge six times, the concentration of SOF_2 rose above 50 ppm, a value that can be detected easily. At the pin-plate electrodes distance of 9 mm, after flashover discharge six times, the concentration of SOF_2 rose closely to 300 ppm. Thus, longer pin-plate electrodes distance may facilitate the generation of characteristic gas. After flashover discharge 15 times, the SOF_2 concentration was almost twice the CF_4 concentration, whereas other gas byproducts increased at slow rates.

3.2.1. Analysis of SOF_2 and SO_2F_2

The concentration of SOF_2 and SO_2F_2 vs. flashover discharge times at different discharge distance were shown in Figure 6. The data indicate that SOF_2 and SO_2F_2 generated steadily as the discharge times increased, and the concentration of SOF_2 was nearly 100 times as high as that of SO_2F_2 . After 6 times flashover discharge, SOF_2 reached almost 300 ppm, while SO_2F_2 was still below 3 ppm. The concentration of SO_2F_2 did not reach 10 ppm before 21 discharge times, however, the SOF_2 concentration exceeded 1000 ppm at this discharge time point. It was also found that as the discharge distance increased, the content of both SOF_2 and SO_2F_2 elevated.



Dominant reaction pathways for SOF_2 and SO_2F_2 were described in Equations (1)–(5). As reported previously, when partial discharge happened in SF_6 atmosphere involving no solid insulation materials, SOF_2 and SO_2F_2 concentration increased at similar rates [13,26]. However, in our experiment, the SO_2F_2 concentration remained far below the SOF_2 concentration. Therefore, flashover discharge happening on epoxy resin may cause a different chemical reaction pathway to facilitate SOF_2 generation.

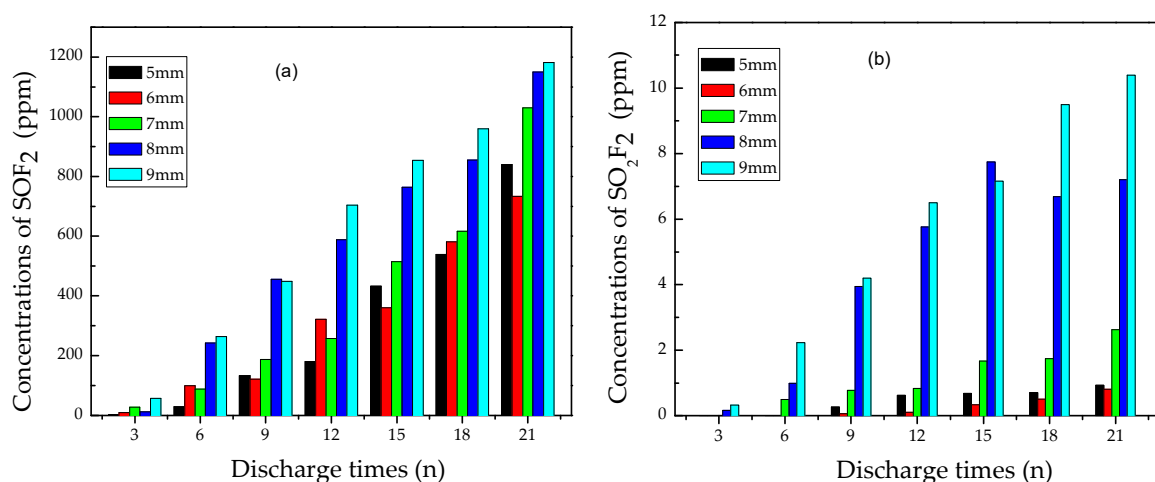


Figure 6. Concentration variation of (a) SOF_2 and (b) SO_2F_2 vs. flashover discharge times.

Actually, under high-energy electron collision, electron-impact-induced dissociation of SF_6 can lead to fluoride sulfide generation such as SF_5 , SF_4 , SF_3 , SF_2 , SF , and so on. It was reported that the amount of SF_4 and SF_2 was larger than that of other gas byproducts [26,27]. When SF_4 comes into contact with H_2O , SOF_2 will soon form, as illustrated in Equation (2). SF_2 can also be oxidized easily into SOF_2 because S atoms of +2 valence can be turned to S atoms of +4 valence during reaction with

high-active O atoms from arc discharge as shown in Equation (1). Therefore, it is reasonable to mark it as an indicator for flashover discharge fault on solid insulation surface.

Generation of SO_2F_2 is more complicated than that of SOF_2 . From the chemical perspective, the S atom in SOF_2 molecule is +4 valence, that means the unsaturated chemical valence needs further oxidation to turn into SO_2F_2 that has an S atom of +6 valence. On the other hand, SF_4 can be oxidized into SOF_4 , then SOF_4 contacts with H_2O to generate SO_2F_2 molecules, which is the main generation resource of SO_2F_2 , as indicated in Equations (4) and (5) [28].

To sum up, SOF_2 was a generated from the reaction between SF_4 and H_2O , while SO_2F_2 mainly comes from the reaction between SOF_4 and H_2O . SOF_4 needs further oxidization of SF_4 by activating O atoms. So the generation of SOF_2 is easier than that of SO_2F_2 . In our study, another characteristic gas CO_2 was generated and its amount increased steadily with the increase of flashover discharge times. The generation of CO_2 can consume a large number of active O atoms, so the SO_2F_2 generation became more difficult under flashover discharge happening on the epoxy resin surface, compared with partial discharge in the SF_6 atmosphere involving no epoxy resin. As a result, the production of SO_2F_2 increased at a quite low rate with flashover discharge times increasing.

Without reckoning the effect of impurities such as H_2O or O_2 in the original SF_6 , epoxy resin decomposition may produce a small amount of water under flashover discharge, which acts as a main factor for Equation (2). Furthermore, H_2O would decompose and release O_2 under imposition of high-current, so Equation (1) also contributes to the generation of SOF_2 . Hence, the concentration of SOF_2 rose rapidly as discharge continued.

3.2.2. Analysis of SO_2

Figure 7 shows the concentration variation of SO_2 vs. discharge times at different pin-plate electrodes distances. At the beginning, the amount of SO_2 was quite small, around 5 ppm after flashover discharge six times. Later, SO_2 was generated steadily as discharge continued, and its concentration reached to about 30 ppm and 55 ppm after discharging 12 times and 21 times, respectively. In addition, the concentration of SO_2 also elevated with the discharge distance increasing.



To better explain the concentration variation of SO_2 , the generation path of SO_2 is depicted in Equations (6)–(9) [29]. It can be seen that the production of SO_2 needs oxygen or water. It is extensively accepted that F atom has stronger reducibility than O atom, but the structure of SO_2 ($\text{O}=\text{S}=\text{O}$) is more symmetrical than that of SOF_2 . Therefore, it is also easy for the generation of SO_2 .

During the reactions, the amount of H_2O was limited, and most of H_2O reacted with subfluorides to form SOF_2 , so there is less amount of H_2O for the generation of SO_2 in Equation (7). Besides, there were very few S atoms provided for the Equation (6) reaction, since S atom is not the main decomposition byproduct of SF_6 . As a result, the content of SO_2 was quite low at the beginning. As discharge continued, S and SF accumulated and had more chances to react with O_2 and H_2O . Thus, after about discharging nine times, the SO_2 concentration reached a high level and increased steadily.

In conclusion, SO_2 began to generate after a certain amount of SF_6 decomposed into S or SF, indicating that SF_6 has already lost its original dielectric property. In order to take SO_2 into consideration for the flashover discharge fault diagnosis method, it is better to take the total concentration of SOF_2 and SO_2 as an indicator for flashover discharge fault.

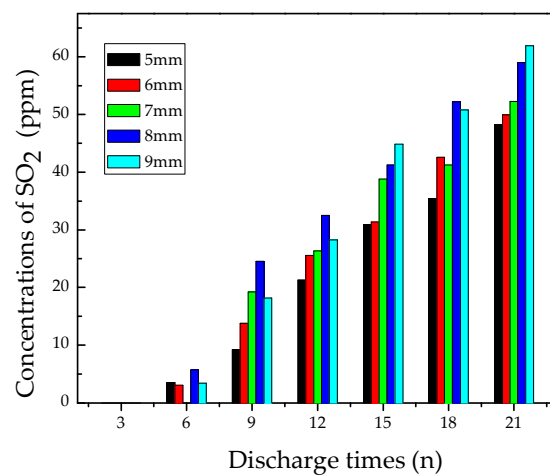


Figure 7. Concentration variation of SO₂.

3.2.3. Analysis of CO₂ and CF₄

Figure 8 shows the concentration variation of CO₂ and CF₄ vs. discharge times under different distances. Both of them were produced once the flashover discharge occurred. After discharging six times, the concentration of CO₂ reached about 10 ppm, while CF₄ exceeded 50 ppm. After discharging 21 times, CF₄ concentration reached over 400 ppm, yet CO₂ concentration was still below 90 ppm, which means that the amount of CF₄ was nearly five times as large as that of CO₂.

CF₄ is an important gas byproduct involved in solid insulation materials decomposition defects. When flashover discharge occurred on epoxy resin, methyl fragments (CH_x) were produced. Through substitution reaction with free F atoms, CH_x would be turned into CF₄. Flashover discharge provided enough energy for the formation of CF₄, whereas CO₂ mainly came from intrinsic decomposition of epoxy resin. So the concentration of CF₄ was much higher than that of CO₂.

In conclusion, CF₄ has a close relationship with epoxy resin decomposition, which can indicate the occurrence of flashover discharge fault on epoxy resin dielectrics in SF₆ insulation equipment. Therefore, the concentration of CF₄ should be monitored intensely.

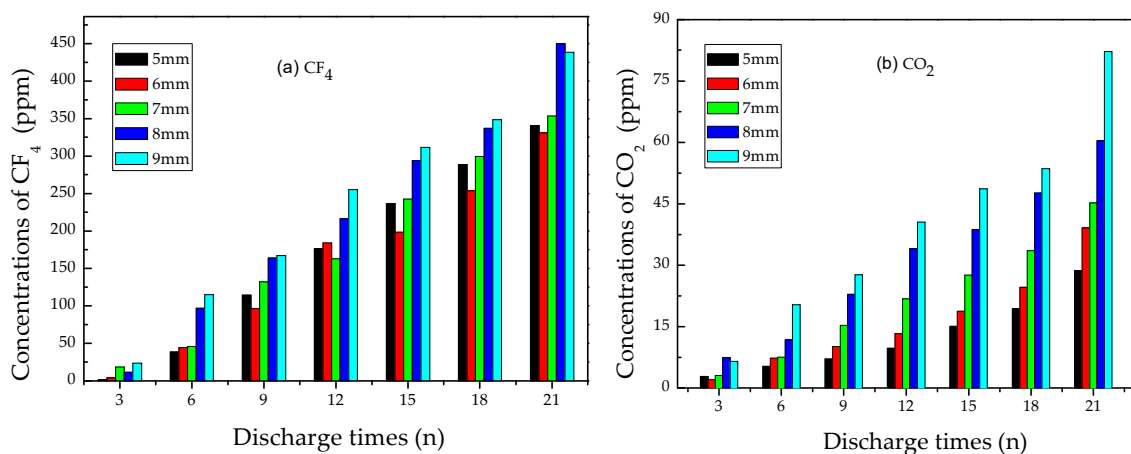


Figure 8. Concentration variation of (a) CF₄ and (b) CO₂.

3.2.4. Analysis of CS₂

Figure 9 shows the concentration changes of CS₂. It can be seen that the content of CS₂ did not reach 3 ppm until discharging 10–15 times. As the discharge times increased, the CS₂ amount grew slowly. After discharging 21 times, the maximum concentration of CS₂ was still less than 6 ppm.

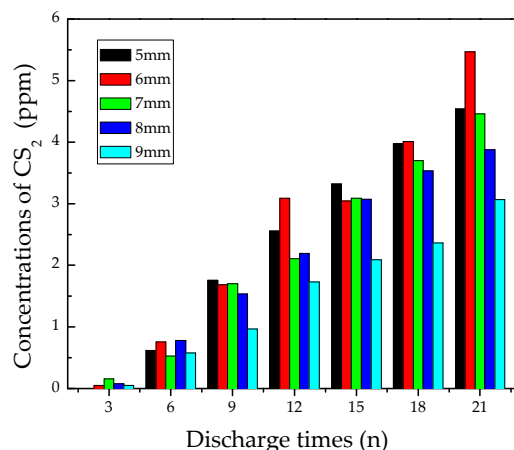


Figure 9. Concentration variation of CS₂.

The generation of CS₂ is difficult because its generation needs active C atoms and S atoms [14,27,28]. On one hand, the amount of C atoms from the decomposition of epoxy resin was limited. The formation of SO₂ also consumed some S atoms, so the remaining amount of S atoms from SF₆ ionization was too low to facilitate the formation of CS₂. C atoms mainly came from ionization of epoxy resin decomposition, and a large number of C atoms were required by the formation of CO₂ and CF₄, so the existing amount of CS₂ was quite low. Besides, the 9 mm gap distance also contributed to the formation of CS₂ to some extent.

As one of the typical byproducts of flashover discharging on epoxy resin dielectrics, CS₂ is too difficult to be generated in comparison with CF₄. Therefore, the appearance of CS₂ could indicate the severest stage of flashover discharge.

3.2.5. Analysis of H₂S

Figure 10 shows the concentration variation of H₂S vs. discharge times at different pin-plate electrodes distances. The results show that the concentration of H₂S was less than 0.3 ppm after discharging nine times, and its concentration only reached 1 ppm after discharging 15 times. After discharging 21 times, its concentration was about 2.5 ppm. A conclusion can be drawn that, like CS₂, the generation of H₂S is as difficult as that of CS₂ among the seven characteristic gases.

The generation of H₂S requires active S atoms and free H atoms [14,28,29]. The S atom is not the main decomposition byproduct of SF₆ [26], and the rising concentration of SO₂ could also reduce the reaction between S atoms and free H atoms. Therefore, the amount of H₂S was extremely small. Although the longer distance between the electrodes can facilitate the generation of H₂S, its amount still stayed at a very low level.

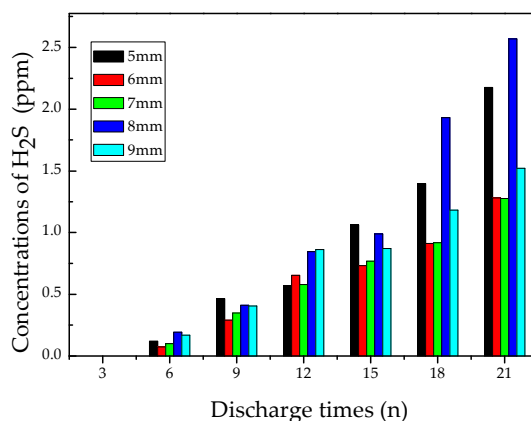


Figure 10. Concentration variation of H₂S.

In conclusion, the generation of H₂S can also be used as an indicator to judge the serious stage of flashover discharge faults on epoxy resin.

3.3. Basic Rules for Judging the Happening of Flashover Discharge

Based on the concentration variation of seven different characteristic gases above, it can be seen that SOF₂ and CF₄ had the highest concentration far beyond other gas byproducts, both of which can therefore represent the main decomposition component resulting from flashover discharge happening on the epoxy resin surface. Compared with the previous studies focusing on partial discharge in SF₆ insulation equipment [1,14,17,24,29], flashover discharge on the epoxy resin surface could cause a drastically elevation in the concentration of SOF₂ and CF₄, but generated a relatively lower concentration for H₂S. According to these two statistics' data, a preliminary rule can be summarized as follows:

$$c_{\text{SOF}_2} > 2c_{\text{CF}_4} \text{ and } (c_{\text{SOF}_2} + c_{\text{CF}_4}) > 400c_{\text{H}_2\text{S}} \quad (10)$$

among which, *c* represents concentration for the selected gases. That is to say, when concentration of SOF₂ reaches twice of that of CF₄, and the sum concentration of both SOF₂ and CF₄ is much higher than that of H₂S, a possible flashover discharge on the epoxy resin surface in SF₆-infused electrical equipment occurs.

3.4. Simulation for Decomposition of Epoxy Resin under High Energy

To verify whether H₂O mainly comes from decomposition of epoxy resin, simulation methods were employed to further investigate decomposition of epoxy resin under high energy. For the sake of simplification, the energy for epoxy resin decomposition was supplied via temperature setting. The whole simulation was conducted with the ReaxFF program and NVT ensemble. NVT represents the three parameters (number (N), volume (V), and temperature (T)) that are fixed parameters, and the other two parameters (pressure (P) and energy (E)) are variables.

Firstly, a ball-stick model of the curing agent molecule was given in Figure 11. After curing, a bisphenol-A epoxy resin (DGEBA) molecule with polymerization degree of 0 was built, as shown in Figure 12. Then, a periodic unit cell of epoxy resin consisting of 20 epoxy resin molecules was constructed with an initial density of 0.5 g/cm³ in a 23.2 Å × 23.2 Å × 23.2 Å cubic box, as shown in Figure 13. The structure was treated by annealing process at the cooling rate of 10 K/500 ps and Energy Minimization and Geometry Optimization were carried out before the decomposition simulation began. The final density of the epoxy resin model was 1.13 g/cm³.

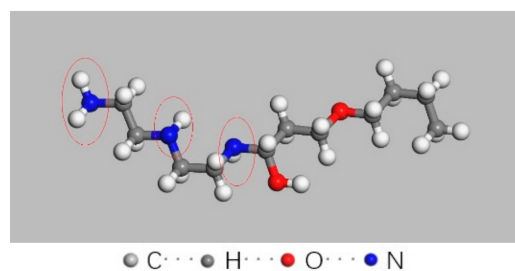


Figure 11. Structure of a single molecule of 593 type curing agent.

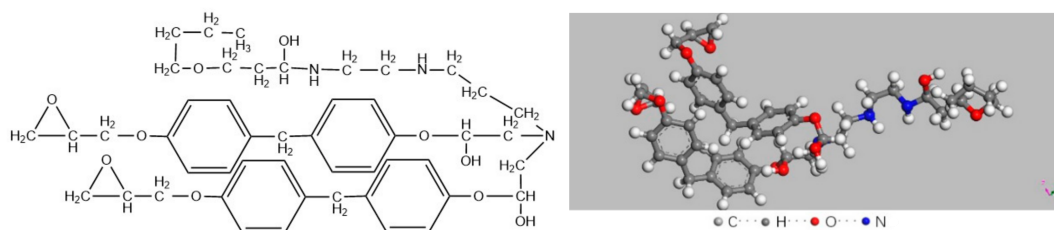


Figure 12. Chemical structure and ball-stick model of an epoxy resin molecule.

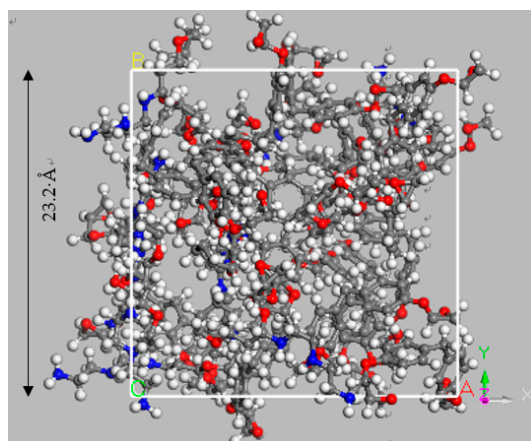


Figure 13. Periodic cubic box of epoxy resin molecules.

The reaction temperature was set at 1300 K to ensure that energy was high enough for epoxy resin decomposition within a total simulation time of 1000 ps [30]. It is already known that the main small molecular products are CH_2O , H_2O , CO , CO_2 , CH_4 , and H_2 [30]. Figure 14 shows the number change of fragments from the periodic unit cell of epoxy resin as a function of time. It can be seen that the number of H_2O molecules was the highest among the 6 byproducts, followed by H_2 , CO_2 , CH_2O , CO , and CH_4 . The dominant reaction pathways (RPWs) of H_2O were shown in Figure 15. CH_4 was mainly derived from demethylation of methyl-group-containing fragments, and H_2 was mainly produced by free hydrogen derived from C-H bond.

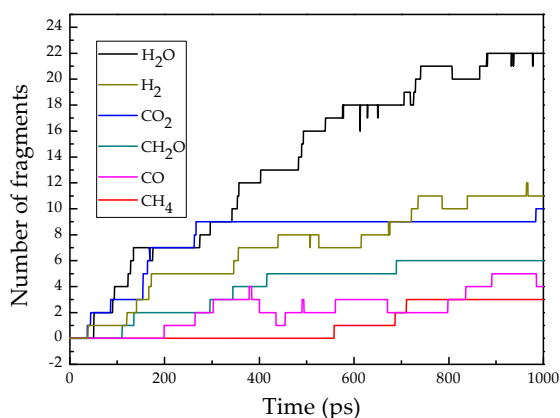


Figure 14. Theoretical number of fragments for the decomposition of epoxy resin heated at 1300 K over time.

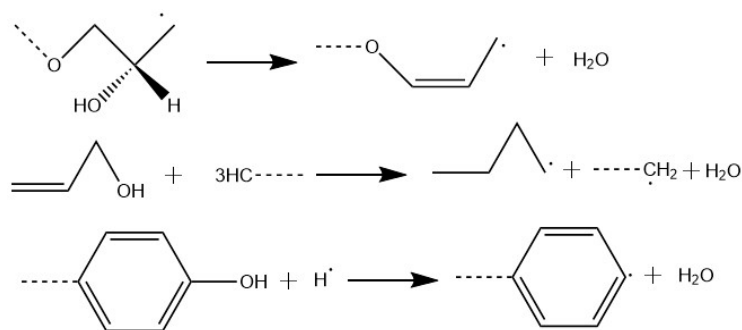


Figure 15. Dominant reaction pathways (RPWs) of H_2O .

In conclusion, epoxy resin could produce H_2O , CH_4 , CO_2 and H_2 that would mainly affect the concentration of seven characteristic gases. H_2O could facilitate the formation of SOF_2 according to

Equations (1)–(3), and CH_4 could facilitate the formation of CF_4 through substitution reaction under high-energy arc discharge. CF_4 decomposed from SF_6 can react with H_2O to form SOF_2 , leading to significantly higher concentration of SOF_2 than other decomposition byproducts. Although the theoretical amount of CH_4 from decomposition of epoxy resin unit cell was relatively lower, F atoms during ionization of SF_6 can help intensify the chemical reaction changing CH_4 to CF_4 under arc discharge; in addition, the C-F bond in the surface structure of fluorinated epoxy resin may also break to form CF_4 directly. Taken together, CF_4 had the second highest concentration during flashover discharge happening on the surface of epoxy resin.

4. Conclusions

In the present study, flashover discharge experiments were carried out on the epoxy resin surface in SF_6 different pin-plate electrodes distances. The concentration of seven characteristic gases including SOF_2 , SO_2 , CF_4 , CO_2 , SO_2F_2 , CS_2 , and H_2S were measured. The following conclusions can be drawn:

Initial flashover discharge voltage decreased sharply in the first three times of flashover discharge, and the discharge voltage fluctuated in a downward tendency.

The concentration of the seven characteristic gases elevated with the flashover discharge times increasing, and the final concentration from high to low follows the order: $\text{SOF}_2 > \text{CF}_4 > \text{SO}_2 > \text{CO}_2 > \text{SO}_2\text{F}_2 > \text{CS}_2 > \text{H}_2\text{S}$. Among these gases, the concentration of SOF_2 and CF_4 was obviously higher than that of other gases. In addition, the concentration of SO_2F_2 , CS_2 , and H_2S kept below 10 ppm after discharging 21 times. Based on the concentration variation of seven characteristic gases, a preliminary rule can be proposed: When the concentration of SOF_2 reaches two times of that of CF_4 , and the sum concentration of both SOF_2 and CF_4 is 400 times higher than that of H_2S , a possible flashover discharge on the epoxy resin surface in SF_6 -infused electrical equipment occurs.

The simulation for decomposition of epoxy resin on the ReaxFF program showed that epoxy resin could produce H_2O , CH_4 , CO_2 , and H_2 that would drastically affect the concentration of the seven characteristic gases. More specifically, H_2O could facilitate the formation of SOF_2 , and CH_4 could react with subfluorides to form CF_4 under high-energy arc discharge.

Author Contributions: Data curation, H.W.; Formal analysis, H.W.; Methodology, H.W., X.Z., R.X. and Y.W.; Project administration, H.W., G.H. and Y.W.; Supervision, X.Z. and R.X.; Writing – original draft, H.W. and G.H.; Writing – review & editing, H.W. and X.Z.

Funding: This research was funded by the National Key R&D Program of China with grant number (2017YFB0903805) and the APC was funded by Wuhan University.

Conflicts of Interest: The authors declare no conflicts of interest.

References

1. Qi, B.; Li, C.; Xing, Z.; Wei, Z. Partial Discharge Initiated by Free Moving Metallic Particles on GIS Insulator Surface: Severity Diagnosis and Assessment. *IEEE Trans. Dielectr. Electr. Insul.* **2014**, *21*, 766–774. [[CrossRef](#)]
2. Albano, M.; Haddad, A.; Griffiths, H.; Coventry, P. Environmentally Friendly Compact Air-Insulated High-Voltage Substations. *Energies* **2018**, *11*, 2492. [[CrossRef](#)]
3. Okubo, H. Recent activity and future trend on ageing characteristics of electrical insulation in GIS from manufacturer's view point. In *Proceedings of 1994 4th International Conference on Properties and Applications of Dielectric Materials (ICPADM), Brisbane, Australia, 3–8 July 1994*; IEEE: Piscataway, NJ, USA, 1994; Volume 2, pp. 837–840.
4. Eriksson, A.; Pettersson, K.G.; Krenicky, A.; Baker, R.; Ochoa, J.R.; Leibold, A. Experience with gas insulated substations in the USA. *IEEE Trans. Power Deliv.* **1994**, *10*, 210–218. [[CrossRef](#)]
5. Piemontesi, M.; Niemeyer, L. (Eds.) Sorption of SF_6 and SF_6 decomposition products by activated alumina and molecular sieve 13X. In *Proceedings of Conference Record of the 1996 IEEE International Symposium on Electrical Insulation, Montreal, QC, Canada, 16–19 June 1996*; IEEE: Piscataway, NJ, USA, 1996; Volume 2, pp. 828–838.

6. Beyer, C.; Jenett, H.; Klockow, D. Influence of reactive SF_x gases on electrode surfaces after electrical discharges under SF₆ atmosphere. *IEEE Trans. Dielectr. Electr. Insul.* **2000**, *7*, 234–240. [[CrossRef](#)]
7. Qiu, Y.; Kuffel, E. Comparison of SF₆/N₂ and SF₆/CO₂ gas mixtures as alternatives to SF₆ gas. *IEEE Trans. Dielectr. Electr. Insul.* **1999**, *6*, 892–895. [[CrossRef](#)]
8. Tang, J.; Liu, F.; Zhang, X.X.; Ren, X.L. Characteristics of the Concentration Ratio of SO₂F₂ to SOF₂ as the Decomposition Products of SF₆ Under Corona Discharge. *IEEE Trans. Plasma Sci.* **2012**, *40*, 56–63. [[CrossRef](#)]
9. Tang, J.; Pan, J.; Yao, Q.; Miao, Y.; Huang, X.; Zeng, F. Feature extraction of SF₆ thermal decomposition characteristics to diagnose overheating fault. *IET Sci. Meas. Technol. L* **2015**, *9*, 751–757. [[CrossRef](#)]
10. Tang, J.; Rao, X.; Tang, B.; Liu, X.; Gong, X.; Zeng, F.; Yao, Q. Investigation on SF₆ spark decomposition characteristics under different pressures. *IEEE Trans. Dielectr. Electr. Insul.* **2017**, *24*, 2066–2075. [[CrossRef](#)]
11. Sauers, I. Evidence for SF₄ and SF₂ formation in SF₆ corona discharges. Presented at the Electrical Insulation and Dielectric Phenomena Conference, Knoxville, TN, USA, 20–24 October 1991.
12. Dourdour, A.; Casanovas, J.; Grob, R.; Mathieu, J. Spark decomposition of SF₆/H₂O mixtures. *IEEE Trans. Electr. Insul.* **1990**, *24*, 1147–1157. [[CrossRef](#)]
13. Sauers, I.; Christophorou, L.G.; Spyrou, S.M. Negative ion formation in compounds relevant to SF₆ decomposition in electrical discharges. *Plasma Chem. Plasma Process.* **1993**, *13*, 17–35. [[CrossRef](#)]
14. Tang, J.; Liu, F.; Zhang, X.; Meng, Q.; Zhou, J. Partial discharge recognition through an analysis of SF₆ decomposition products part 1: Decomposition characteristics of SF₆ under four different partial discharges. *IEEE Trans. Dielectr. Electr. Insul.* **2012**, *19*, 29–36. [[CrossRef](#)]
15. Belmadani, B.; Casanovas, J.; Casanovas, A.M. SF₆ decomposition under power arcs. II. Chemical aspects. *IEEE Trans. Electr. Insul.* **1991**, *26*, 1177–1182. [[CrossRef](#)]
16. Chu, F.Y. SF₆ Decomposition in Gas-Insulated Equipment. *IEEE Trans. Electr. Insul.* **1986**, *21*, 693–725. [[CrossRef](#)]
17. Hergli, R.; Casanovas, J.; Dourdour, A.; Grob, R.; Mathieu, J. Study of the Decomposition of SF₆ in the Presence of Water, Subjected to Gamma Irradiation or Corona Discharges. *IEEE Trans. Electr. Insul.* **2002**, *23*, 451–465. [[CrossRef](#)]
18. Griffin, G.D.; Sauers, I.; Kurka, K.; Easterly, C.E. Spark decomposition of SF₆: Chemical and biological studies. *IEEE Trans. Power Deliv.* **1989**, *4*, 1541–1551. [[CrossRef](#)]
19. Chen, J.; Zhou, W.; Yu, J.; Su, Q.; Zheng, X.; Zhou, Y.; Li, L.; Yao, W.; Wang, B.; Hu, H. Insulation condition monitoring of epoxy spacers in GIS using a decomposed gas CS₂. *IEEE Trans. Dielectr. Electr. Insul.* **2013**, *20*, 2152–2157. [[CrossRef](#)]
20. Zhang, Y.; Rhee, K.Y.; Park, S.-J. Nanodiamond nanocluster-decorated graphene oxide/epoxy nanocomposites with enhanced mechanical behavior and thermal stability. *Compos. B Eng.* **2017**, *114*, 111–120. [[CrossRef](#)]
21. Zhang, Y.; Choi, J.R.; Park, S.-J. Thermal conductivity and thermo-physical properties of nanodiamond-attached exfoliated hexagonal boron nitride/epoxy nanocomposites for microelectronics. *Compos. Part A: Appl. Sci. Manuf.* **2017**, *101*, 227–236. [[CrossRef](#)]
22. Zhang, Y.; Heo, Y.-J.; Son, Y.-R.; In, I.; An, K.-H.; Kim, B.-J.; Park, S.-J. Recent advanced thermal interfacial materials: A review of conducting mechanisms and parameters of carbon materials. *Carbon* **2019**, *142*, 445–460. [[CrossRef](#)]
23. Tang, J.; Zeng, F.P.; Pan, J.Y.; Zhang, X.X. Correlation Analysis between Formation Process of SF₆ Decomposed Components and Partial Discharge Qualities. *IEEE Trans. Dielectr. Electr. Insul.* **2013**, *20*, 864–876. [[CrossRef](#)]
24. Fukunaga, K.; Takai, H. Deterioration of epoxy resin as a result of internal partial discharge. *Electr. Eng. Jpn.* **2010**, *111*, 11–19. [[CrossRef](#)]
25. Xie, Q.; Liu, X.; Zhang, C.; Wang, R.; Rao, Z.; Shao, T. Aging Characteristics on Epoxy Resin Surface Under Repetitive Microsecond Pulses in Air at Atmospheric Pressure. *Plasma Sci. Technol.* **2016**, *18*, 325–330. [[CrossRef](#)]
26. Brunt, R.J.V.; Sauers, I. Gas-phase hydrolysis of SOF₂ and SOF₄. *J. Chem. Phys.* **1986**, *85*, 4377–4380. [[CrossRef](#)]
27. Brunt, R.J.V.; Herron, J.T. Plasma chemical model for decomposition of SF₆ in a negative glow corona discharge. *Phys. Scr.* **1994**, *T53*, 9. [[CrossRef](#)]
28. Fan, L.; Ju, T.; Liu, Y. Mathematical model of influence of oxygen and moisture on feature concentration ratios of SF₆ Decomposition Products. In Proceedings of the 2012 IEEE Power and Energy Society General Meeting, San Diego, CA, USA, 22–26 July 2012; pp. 1–5.

29. Zeng, F.; Tang, J.; Zhang, X.; Sun, H.; Yao, Q.; Miao, Y. Study on the influence mechanism of trace H₂O on SF₆ thermal decomposition characteristic components. *IEEE Trans. Dielectr. Electr. Insul.* **2017**, *24*, 367–374. [[CrossRef](#)]
30. Diao, Z.; Zhao, Y.; Chen, B.; Duan, C.; Song, S. ReaxFF reactive force field for molecular dynamics simulations of epoxy resin thermal decomposition with model compound. *J. Anal. Appl. pyrolysis* **2013**, *104*, 618–624. [[CrossRef](#)]



© 2019 by the authors. Licensee MDPI, Basel, Switzerland. This article is an open access article distributed under the terms and conditions of the Creative Commons Attribution (CC BY) license (<http://creativecommons.org/licenses/by/4.0/>).